Direct verification of Ga–Ga bond avoidance in the type-I clathrate $Ba_8Ga_{16}Sn_{30}$ from its x-ray absorption fine structure

M. Kozina,[1] F. Bridges,[1] Y. Jiang,[1] M. A. Avila,[2] K. Suekuni,[3] and T. Takabatake[3]
[1]*Physics Department, University of California, Santa Cruz, California 95064, USA*
[2]*Centro de Ciências Naturais e Humanas, Universidade Federal do ABC, Santo André 09210-170, SP, Brazil*
[3]*Department of Quantum Matter, ADSM, Hiroshima University, Higashi, Hiroshima 739-8530, Japan*
(Received 18 August 2009; revised manuscript received 16 October 2009; published 16 December 2009)

Experiments in the past have only been able to suggest that Ga–Ga bonds are not favored in the cage structure of $Ba_8Ga_{16}Sn_{30}$ and other type-I clathrates. Here we show definitive evidence that this is indeed the case. Using the extended x-ray-absorption fine structure technique, we are able compare the backscattering functions for the first neighbors about Ga to the calculated functions for Ga–Ga and Ga–Sn bonds. The result is that only ~15% of the Ga nearest neighbors are Ga. Combining this result with diffraction data on occupational parameters, we propose one possible arrangement of Ga and Sn in the unit cell of $Ba_8Ga_{16}Sn_{30}$. Additionally, we find significant disorder in the Ga/Sn lattice; the Ga–Sn bond is 0.07 Å and the Ga–Ga 0.2 Å shorter than the average bond length, which must contribute to the smaller thermal conductivity.

DOI: 10.1103/PhysRevB.80.212101 PACS number(s): 61.66.Fn, 82.75.−z, 72.15.Jf, 61.05.cj

The type-I clathrates $X_8Ga_{16}Ge_{30}$ (X=Ba, Sr, and Eu)[1,2] and recently $Ba_8Ga_{16}Sn_{30}$ (Ref. 3) have the unusual properties that the electrical conductivity is moderately good but the thermal conductivity is poor, nearly glasslike; consequently they come close to the electron-crystal/phonon-glass concept proposed by Slack[4] for good thermoelectric materials. These compounds are compensated semiconductors and for some systems the charge-carrier type can be changed from n type to p type with a small variation in the Ga:Ge or Ga:Sn ratio. Unlike the type-VIII clathrate form of $Ba_8Ga_{16}Sn_{30}$, which exhibits significant differences in the temperature dependence of the thermal conductivity (κ) between p type and n type, the type-I form considered here, shows only a small difference in κ between p type and n type.[5] However, κ for the n type is consistently slightly larger than that found in the p type.

The structure of the type-I clathrates (X_8M_{46}) consists of two connected cages—a 20-atom cage (M20) and a 24-atom cage (M24). There are three crystallographic sites within this cage structure occupied by Ga/Ge or Ga/Sn atoms—M1 (6c site), M2 (16i site), and M3 (24k site). The X atoms are located near the centers of each of the two cages and it is believed that the low-frequency "rattling" motion of X atoms, such as Eu and Sr, provides the main phonon scattering mechanism, but the coupling between the higher energy phonon vibrations in the cage structure and the X rattlers is more difficult to quantify. For $Ba_8Ga_{16}Ge_{30}$, the situation is less clear[6,7] as in this clathrate the Ba2 off-center displacement in the M24 cage is small,[6,8] the results appear to be sample dependent, and disorder within the lattice cages may be important.[6,7] However for $Ba_8Ga_{16}Sn_{30}$, considered here, Ba2 also has a large off-center displacement.[5]

It has long been recognized that the distribution of Ga on the three sites is not random,[9–11] and the distribution may be important in determining the rattler-cage phonon coupling.[8] One suggestion is that the structure minimizes the number of Ga–Ga bonds—i.e., the group III element, Ga, prefers to have nearest-neighbor Ge or Sn neighbors.[9,12] Distributions of Ga on the three sites M1-M3 from diffraction are generally consistent with such a model[5,10] but to date there is no direct proof. Here we show directly, from the shape of the extended x-ray-absorption fine structure (EXAFS) spectra in r space (without any fitting) that the nearest neighbors to Ga in $Ba_8Ga_{16}Sn_{30}$ are, in fact, primarily Sn.

The EXAFS function for $k\chi(k)$ is a sum over neighboring shells and is given by (see Ref. 8)

$$k\chi(k) = \sum_i k\chi_i(k) = \mathrm{Im}\sum_i A_i \int_0^\infty F_i(k,r)\frac{g_i(r_{0i},r)e^{i[2kr+2\delta_c(k)+\delta_i(k)]}}{r^2}dr. \quad (1)$$

The backscattering amplitude F_i of a high-energy, x-ray ejected photoelectron depends on the atomic number Z of the backscattering atom, and if ΔZ for two different types of backscattering atoms is sufficiently large, the type of backscatterer can be determined. Further, as Z increases there are more Ramsauer-Townsend-type resonances,[13,14] which significantly change the shape of the nearest-neighbor peak in r space. For $Ba_8Ga_{16}Ge_{30}$, ΔZ=1 for Ga and Ge, so there is essentially no contrast. However for $Ba_8Ga_{16}Sn_{30}$, ΔZ=19 between Ga and Sn, and the contrast is high.

Using the program FEFF,[15] we have calculated the theoretical EXAFS functions $[k\chi(k)]$, at the Ga K edge, for the Ga–Ga and Ga–Sn nearest-neighbor pairs. The shape of the functions are strongly determined by the backscattering amplitude function, $F(k,r)$. In Fig. 1(a) we plot the Fourier transform (FT) of $k\chi(k)$, FT$[k\chi(k)]$, as a function of r for the Ga–Ga pair; the fast oscillation is the real part, R, of the FT and the envelope function is $\pm\sqrt{R^2+I^2}$, where I is the imaginary part of the FT. In Fig. 1(b) we plot the corresponding function for Sn backscatterers. In these plots we have added a small broadening (σ^2=0.0020 Å^2) typical of many atom pairs at low temperature, and shifted the effective K-edge energy by −7.5 eV to correspond with the experimental edge energy position, defined as the half-height point on the edge

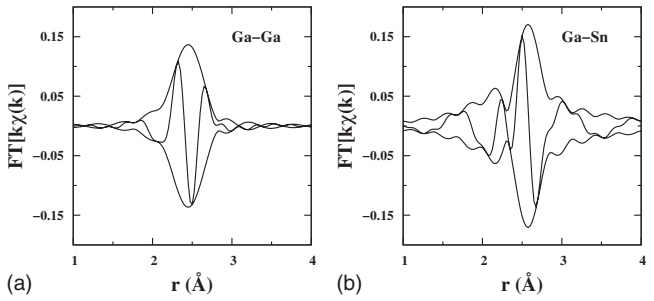

FIG. 1. The theoretical r space function for (a) the Ga–Ga pair and (b) the Ga–Sn pair calculated using FEFF. The FT range is 3.5–14.4 $Å^{-1}$ with a Gaussian rounding of the FT window of 0.3 $Å^{-1}$. For both plots a small broadening (σ^2=0.0020 $Å^2$) was included and E_o was shifted to correspond to the E_o of the data, see text.

(E_o for the theoretical function defines where k=0, near the bottom of the edge). As shown in Fig. 1 the Ga–Ga peak is less spread out, with small tails on either side of the peak; while for Ga–Sn, the peak is much broader, the tails are larger and there is a well-defined dip near 2.3 Å that is missing in the Ga–Ga plot. Thus these two r-space theoretical functions are very different. We will make use of that difference to determine the main type of nearest neighbors to Ga in Ga K-edge EXAFS.

The Ga K-edge EXAFS data were collected at SSRL (Stanford Synchrotron Radiation Lightsource) in transmission mode on beamline 10-2 using a Si 111 double monochromator. The slit height was 0.5 mm, which provided an energy resolution of ~2 eV, and the monochromator was detuned 50% to minimize harmonics.

Single crystals were prepared by Avila *et al.*; see Refs. 3 and 5 for detailed information on the crystal growth. EXAFS samples were made by first grinding the crystals using a mortar and pestle and then passing the powder through a 400 mesh sieve. The resulting fine powder was brushed onto scotch tape. The tape preferentially holds the smaller grains ($\leq$5 μm) in a thin layer. Two layers of tape were pressed together (double layer) to encapsulate the powder. For the Ga K-edge measurements four double layers were used which gave Ga K-edge jumps of 0.4 (n type) and 0.45 (p type).

In Fig. 2(a) we show the Ga K-edge k-space data out to k=15 $Å^{-1}$ for n type $Ba_8Ga_{16}Sn_{30}$ at 4 K. Similar high signal-to-noise data were also obtained for a p-type sample. In Figs. 2(b) and 2(c) we show the Fourier-transformed r-space data (from 3.5–14.4 $Å^{-1}$) for the n- and p-type samples out to 4 Å; the two spectra are very similar. More importantly, a comparison of the first peak, 2–3 Å range, with the theoretical functions for Ga–Ga and Ga–Sn pairs in Fig. 1 shows immediately that the data look nearly identical to the Ga–Sn function and not at all like the Ga–Ga function. Note the dip in the envelope near 2.25 Å and the real parts R of the FT (particularly from 2–2.75 Å) are almost the same in Figs. 1(b), 2(b), and 2(c). This is direct proof that most of the neighbors about Ga are Sn atoms.

To go further and quantify the fraction of Sn neighbors, one must fit the first peak in the data to a sum of the theoretical functions for the Ga–Sn and Ga–Ga pairs, with the total coordination number constrained to correspond to four neighbors. Since the data are so similar to the Ga–Sn function we started the fit with 75% Ga–Sn (i.e., three Sn neighbors) and 25% Ga–Ga. We allowed σ (width of the pair-distribution function) and the bond length r of each pair to vary in the first fits. The fit range was from 1.5 to 3 Å in r space and 3.5 to 14.4 $Å^{-1}$ in k space. Note that the weak Ga–Ba1 peak occurs well above 3.3 Å and does not contribute to this first peak.

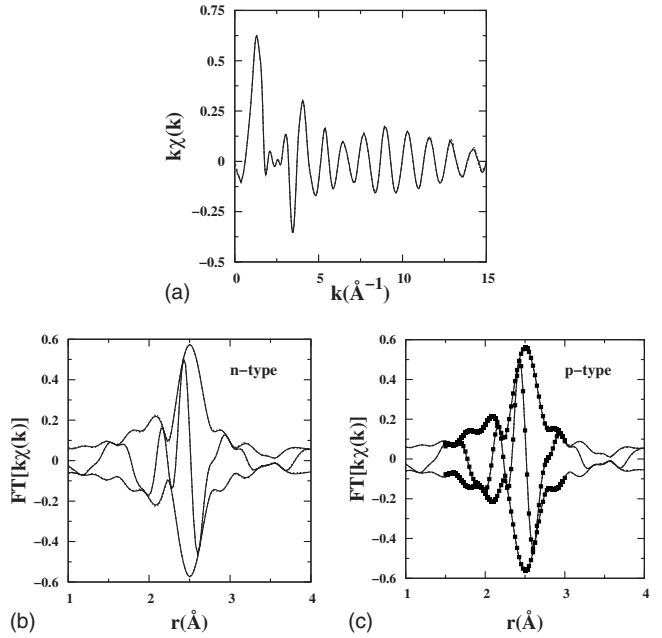

FIG. 2. Ga K-edge data at 4 K for $Ba_8Ga_{16}Sn_{30}$; same FT range as Fig. 1. (a) k-space data (n type); (b) r-space data (n type); and (c) r-space data (p type) along with the fit from 1.5 to 3 Å (squares) (S_o^2 parameter is 0.93). For each plot three traces are overlaid to show the high quality of the data—only above 14 Å in part (a) can one see a tiny difference.

Using further refinements to the fits, we find that in the n type material 85% of the Ga neighbors are Sn and 15% ± 5% are Ga (p type identical), compared to 35% Ga nearest neighbors expected for a random distribution. These fits confirm the visual inspection of Figs. 1 and 2, namely, that the Ga–Ga bonds make up only a small fraction of the nearest-neighbor Ga bonds. This is a direct confirmation of Blake *et al.*'s[12] prediction that the lowest energy configuration has few Ga–Ga pairs.

Our data suggest that there are either four or five Ga–Ga pairs in the unit cell, corresponding to 13% and 16% Ga–Ga, respectively. Using these results in tandem with the occupational parameters measured by Suekuni *et al.*,[5] we were able to construct one possible arrangement of the unit cell (Fig. 3) with four Ga–Ga pairs. Alternatively, by moving the Ga on site A in Fig. 3 to site B we leave the occupational parameters unchanged while adding one more pair of Ga atoms. Most likely there are other configurations as well since the asymmetry within the unit cell (while preserving translational symmetry at the surface) allows for several switches of Ga sites while not violating the occupational parameters.

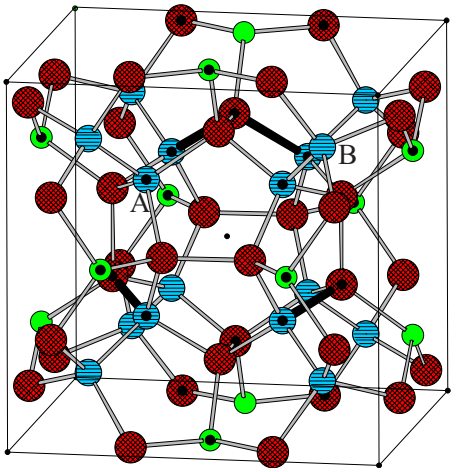

FIG. 3. (Color online) The unit cell of $Ba_8Ga_{16}Sn_{30}$. The small black dots on the corners and in the center are the Ba1 sites. The Ba2 sites are removed for clarity. The largest balls (red with cross-hatches) are the M3 (24*k*) sites. The medium balls (blue with horizontal stripes) are the M2 (16*i*) sites. The small balls (green with no texture) are the M1 (6*c*) sites. A Ga site is marked by a black dot in the center of one of the larger balls. The four Ga–Ga bonds are in black. Site B is an alternate location for the Ga at A; switching these yields one more Ga–Ga pair.

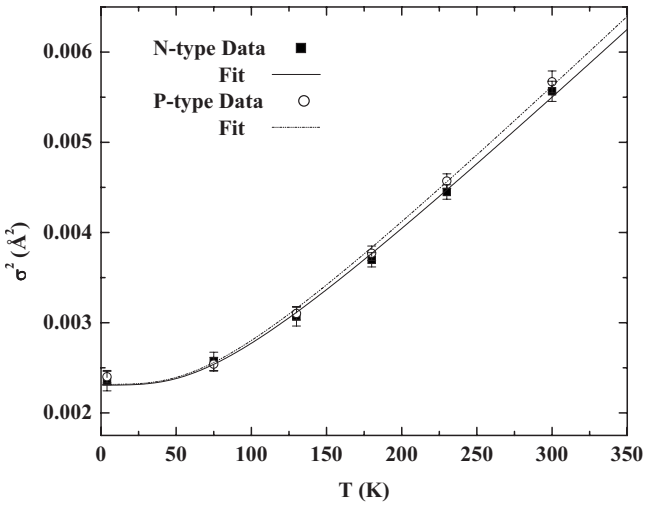

FIG. 4. Temperature dependence of σ^2 for the Ga–Sn bond with a fit to a correlated Debye model. The *n*-type data are shown as solid squares with fit the solid line; the *p*-type data are represented by the empty circles and the fit by the dashed line.

Moreover, from the fits we found both the Ga–Ga and Ga–Sn bond lengths are shorter than the averages calculated using the crystal structure.[3] We started the fit with the average Ga–Ga and Ga–Sn bond length, each 2.73 Å, but the two shifted down to 2.55 and 2.66 Å (*n* type), and 2.54 and 2.66 Å (*p* type), respectively. It is of interest that the Ga–Ga bond shifts down to approximately 2.55 Å, almost 0.2 Å below the average bond length, and closer to the Ga–Ga/Ge bond distances in $Ba_8Ga_{16}Ge_{30}$ (2.50 Å on average).[8,16] This indicates that the Ga–Ga bond length is roughly constant regardless of the other cage atom. A nearly constant Ga–Ga bond length is quite similar to the old study on $Ga_{1-x}In_xAs$ in which the Ga–As distance remains nearly constant although the lattice expands as the fraction of In increases from $x=0$ to 1.[17] The short Ga–Sn bond here also implies that the Sn–Sn distance should be larger than the average bond distance. A preliminary check of one Sn *K*-edge scan is consistent with a larger Sn–Sn bond, but more data are needed. The magnitude of these deviations from the average bond length indicates that the $Ba_8Ga_{16}Sn_{30}$ cage structure is significantly disordered, which must contribute to the smaller thermal conductivity κ found in $Ba_8Ga_{16}Sn_{30}$;[5] it also suggests that the cages might be dimpled.

We fit σ^2 of the Ga–Sn first neighbor bond to a correlated Debye model (see Fig. 4), and found the correlated Debye temperature to be 315 ± 20 K for the *n*-type material and 310 ± 20 K for the *p* type, essentially the same within our errors. This value for the correlated Debye temperature is smaller than that found in $Ba_8Ga_{16}Ge_{30}$ for the Ga–Ga/Ge bond, namely, 410 and 415 K (*n* type and *p* type, respectively).[8] This suggests the Ga–Sn bond is weaker than the average Ga–Ga/Ge bond. We also found the static offsets for the Ga–Sn bond to be 5.7×10^{-4} and 5.5×10^{-4} Å^2, respectively, signifying that the inherent disorder for a given bond does not differ much between the *n*-type and *p*-type materials. However note that these values of the static offsets are on the order of our error.

Our EXAFS data apply only to $Ba_8Ga_{16}Sn_{30}$; however, the fractional occupational parameters of other type-I clathrates containing Ga are roughly similar (see Table I), though the variation is large especially for the 16*i* and 24*k* sites. It seems reasonable, then, to expect the Ga–Ga bonds to be likewise suppressed in other clathrates, even if the actual number of Ga–Ga bonds varies slightly, but it needs to be checked.

Prior experiments were only able to suggest that the number of Ga–Ga bonds are minimized in $Ba_8Ga_{16}Sn_{30}$.[5] However, by means of EXAFS analysis, we are able to tell explicitly that the Ga–Ga bonds make up only a small

TABLE I. Fractional occupational parameters of the Ga atom for several type-I clathrates.

Compound	Method	6*c*	16*i*	24*k*
$Ba_8Ga_{16}Sn_{30}$ (*n* type)[a]	x ray	0.71	0.36	0.25
$Ba_8Ga_{16}Sn_{30}$ (*p* type)[a]	x ray	0.68	0.34	0.26
$Ba_8Ga_{14.6}Si_{31.4}$ [b]	x ray	0.61	0.08	0.40
$Ba_8Ga_{15.7}Si_{30.3}$ [b]	neutron	0.63	0.11	0.43
$Ba_8Ga_{16}Ge_{30}$ (*n* type)[c]	x ray	0.76	0.16	0.37
$Ba_8Ga_{16}Ge_{30}$ (*n* type)[c]	neutron	0.74	0.17	0.37
$Ba_8Ga_{16}Ge_{30}$ (*p* type)[c]	x ray	0.64	0.17	0.39
$Ba_8Ga_{16}Ge_{30}$ (*p* type)[c]	neutron	0.60	0.33	0.30

[a]Reference 5.
[b]Reference 11.
[c]Reference 9.

fraction of the nearest-neighbor Ga bonds. Moreover, our results (specifically that ~15% of the Ga nearest neighbors are Ga) do not conflict with the occupational parameters provided by Suekuni *et al.*[5] but rather allow us to construct a possible arrangement of the Ga and Sn atoms in the unit cell. Thus, it is clear that there is a preferential arrangement of the cage atoms Ga and Sn in $Ba_8Ga_{16}Sn_{30}$.

The work at Hiroshima was supported by Grant-in-Aid for Scientific Research from MEXT of Japan, Grants No. 18204032, No. 19051011, and No. 20102004. The experiments were performed at SSRL (operated by the DOE, Division of Chemical Sciences, and by the NIH, Biomedical Resource Technology Program, Division of Research Resources).

[1] B. C. Sales, B. C. Chakoumakos, R. Jin, J. R. Thompson, and D. Mandrus, Phys. Rev. B **63**, 245113 (2001).
[2] G. S. Nolas, J. L. Cohn, G. A. Slack, and S. B. Schujman, Appl. Phys. Lett. **73**, 178 (1998).
[3] M. A. Avila, K. Suekuni, K. Umeo, H. Fukuoka, S. Yamanaka, and T. Takabatake, Appl. Phys. Lett. **92**, 041901 (2008).
[4] G. A. Slack, in *CRC Handbook of Thermoelectrics*, edited by D. M. Rowe (Chemical Rubber, Boca Raton, FL, 1995), pp. 407–440.
[5] K. Suekuni, M. A. Avila, K. Umeo, H. Fukuoka, S. Yamanaka, T. Nakagawa, and T. Takabatake, Phys. Rev. B **77**, 235119 (2008).
[6] M. Christensen, N. Lock, J. Overgaard, and B. B. Iverson, J. Am. Chem. Soc. **128**, 15657 (2006).
[7] M. Christensen, A. B. Abrahamsen, N. B. Christensen, F. Juranyi, N. H. Anderson, K. Lefmann, J. Andreasson, C. R. H. Bahl, and B. B. Iverson, Nature Mater. **7**, 811 (2008).
[8] Y. Jiang, F. Bridges, M. A. Avila, T. Takabatake, J. Guzman, and G. Kurczveil, Phys. Rev. B **78**, 014111 (2008).
[9] M. Christensen and B. B. Iversen, Chem. Mater. **19**, 4896 (2007).
[10] Y. Zhang, P. Lee, G. Nolas, and A. Wilkinson, Appl. Phys. Lett. **80**, 2931 (2002).
[11] A. Bentien, E. Nishibori, S. Paschen, and B. B. Iversen, Phys. Rev. B **71**, 144107 (2005).
[12] N. P. Blake, D. Bryan, S. Latturner, L. Mollnitz, G. D. Stucky, and H. Metiu, J. Chem. Phys. **114**, 10063 (2001).
[13] G. G. Li, F. Bridges, and C. H. Booth, Phys. Rev. B **52**, 6332 (1995).
[14] M. L. Hanham and R. F. Pettifer, Phys. Rev. B **64**, 180101(R) (2001).
[15] A. L. Ankudinov, B. Ravel, J. J. Rehr, and S. D. Conradson, Phys. Rev. B **58**, 7565 (1998).
[16] B. C. Chakoumakos, B. C. Sales, and D. G. Mandrus, J. Alloys Compd. **322**, 127 (2001).
[17] J. C. Mikkelsen and J. B. Boyce, Phys. Rev. B **28**, 7130 (1983).